Laser and Particle Beams (2005), *23*, 411–416. Printed in the USA.

DOI: 10.1017/S0263034605050585

Evidence of enhanced effective hot electron temperatures in ultraintense laser-solid interactions due to reflexing

HUI CHEN AND SCOTT C. WILKS
Lawrence Livermore National Laboratory, University of California, Livermore, California

(RECEIVED 8 February 2005; ACCEPTED 17 April 2005)

Abstract

It is shown that the effective hot electron temperature, T_{hot}, associated with the energetic electrons produced during the interaction of an ultra-intense laser with thin solid targets is dependent on the thickness of the target. We report the first direct experimental observations of electron energy spectra obtained from laser-solid interactions that indicates the reflexing of electrons in thin targets results in higher electron temperatures than those obtained in thick target interactions. This can occur for targets whose thickness, x_t, is less than about half the range of an electron at the energy associated with the initial effective electron temperature, provided the laser pulse length is at least $c\tau_p > 2x_t$. A simple theoretical model that demonstrates the physical mechanism behind this enhanced heating is presented and the results of computer simulations are used to verify the model.

Keywords: Debye sheath; Femtosecond lasers; Hot electrons; Laser-plasma interaction; Nonlinear ponderomotive force; PIC computations; Target normal sheath acceleration; Target thickness

1. INTRODUCTION

An ultraintense laser pulse (i.e., intensities $I \geq 10^{18}$ W/cm^2 for a laser wavelength of 1 μm) impinging on a solid target, transfers its energy to the material by first generating a population of hot electrons that are picked out of the existing background electron population, that is created near the interaction region. There exists a correlation between the effective temperature of these hot electrons and the incident laser intensity (Wilks *et al*., 1992; Wilks & Kruer, 1997); Kruer & Wilks, 1992). Although the actual temperature is usually somewhat dependent on the plasma scale length near the critical surface (Lefebvre & Bonnaud, 1997; Fuchs *et al*., 1998), the measured effective electron energies from experiment tend to agree with this value. The critical density, $n_{cr} = \gamma\omega_0^2 m_e/(4\pi e^2)$($\omega_0$ = laser frequency; m_e, e = electron mass, charge, $\gamma = (1 - v^2/c^2)^{-1}$ is the relativistic factor required if the electron energy is greater than 511 keV) is defined as the density above which the laser cannot propagate beyond, its energy being either reflected or absorbed at this point. The exact nature of the plasma in this region just in front of the solid surface (i.e., the electron and ion density and temperature) is usually dependent either on the amount of energy in a pre-pulse or the amplified spontaneous emission (ASE), that is, inherent CPA generated short pulse lasers, or both, depending on the magnitude of each (Adumi *et al*., 2004).

It has long been theorized (Liang *et al*., 1998; Shen & Meyer-Ter-Vehn, 2001) that by choosing an appropriate target thickness, x_t, the effective temperature of the electrons produced in the interaction of an ultra-intense laser with this target can be enhanced by electrons reflexing back and forth through the target. Of course, this will only occur provided that the target is thin enough, relative to the laser pulse length (τ_p), such that electrons accelerated at the laser-plasma interface can make the round trip through the target while the laser is still on ($\tau_p < 2^* x_t/c$). Preferably, if the range of the electrons (R_e) is long enough such that the electrons retain most of the energy they had on initial acceleration, and the more round trips, the higher the energy, up to a point. However, this phenomenon has not been directly measured by experiment up to now. Here, we report on direct experimental observations that confirm this hypothesis, and discuss simulations that provide a physical model on which to interpret the results.

2. EXPERIMENTAL RESULTS

The data consist of approximately 25 shots using the JanUSP (Bonlie *et al*., 2000) laser at the Lawrence Livermore National Laboratory in the United States. The JanUSP is a Ti:Sap-

Address correspondence and reprint requests to: Scott S. Wilks, Lawrence Livermore National laboratory, L-209, P.O. Box 808, Livermore, CA, 94550. E-mail: wilks1@llnl.gov

phire laser, run in the unpumped mode where the energy is in the range of $\sim$ 100 mJ. The laser was focused by an f/2 off-axis parabola onto a target whose normal was at 22.5 degrees to the **k**-vector of the incident laser light. The pulse length was $\tau \sim 100$ fs, and the spot size that contained 30–40% of the energy was approximately 4–8 microns full width half maximum (FWHM). This made for intensities $I \sim 10^{18}$ W $\times$ μm^2/cm^2, $\lambda = 0.8$ μm. The laser intensity contrast between the pre-pulse and the peak of the pulse was roughly 10^{10} (Itatani *et al*., 1998). The targets in this study were strips of aluminum or gold with dimensions 20 mm wide by 20 mm long, and thicknesses varying between 2 μm and 100 μm. The electron energies were measured using a fiber array compact electron spectrometer (Chen *et al*., 2003). The spectrometer uses permanent magnets for electron energy dispersion and an array of over 100 scintillating fibers coupled to a 1024 $\times$ 1024 pixel CCD as the detection system. The magnet strength was set to 1000 Gauss, to measure electron energies up to 10 MeV. The spectrometer was oriented normal to the target surface, and looked at electrons escaping from the front of the target (the side that the laser hits) which was approximately 15 cm away.

Typical electron spectra from our measurements are shown in Figure 1 for the case of an aluminum target with thicknesses of 2 μm and 50 μm. The effective electron temperature was derived by fitting the electron energy spectrum to a simple Boltzmann exponential distribution, $\exp(-E/kT_{hot})$, where the highest energies had less weighting, as the signal level fell into the level of the noise. The resulting plot of the effective electron temperature as a function of foil thickness for both Au and Al targets is shown in Figure 2. Also plotted (in open diamonds) are the weighted average temperatures for each measurement taken during the campaign. From this figure, it is clear that the hot electron temperature decreases as the foil thickness increases for both materials.

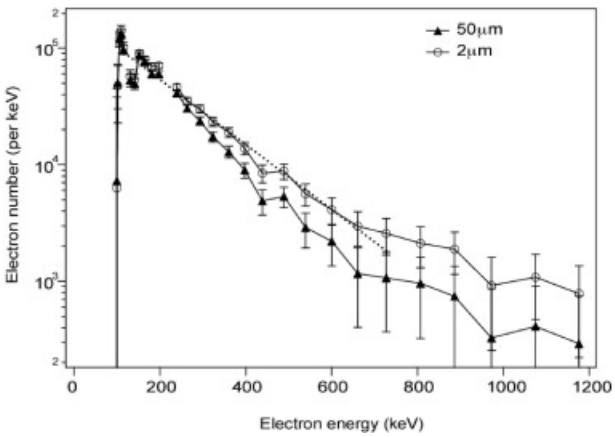

Fig. 1. Electron spectra for two different thicknesses of Al targets taken at the laser intensity of 97 mJ. An electron temperature of about 120 keV was derived for 2 μm thick target (dotted line) to the spectrum, and 100 keV for the 50 μm thick target.

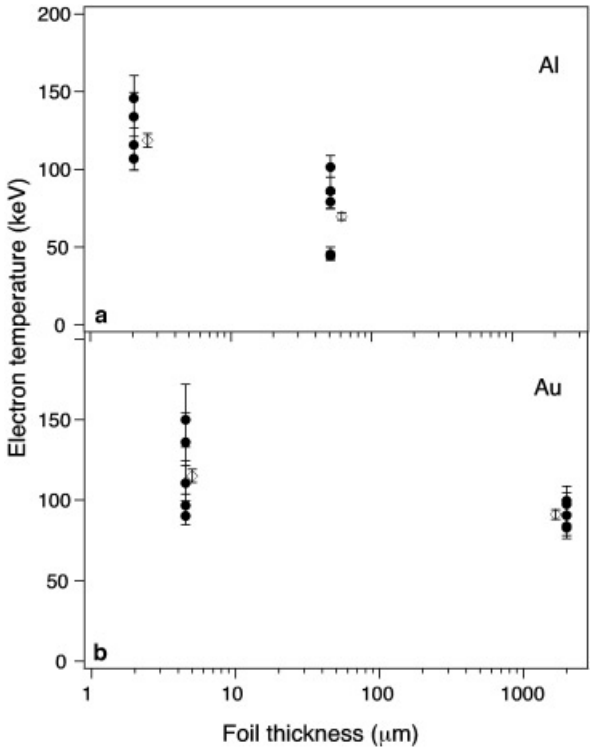

Fig. 2. Electron temperatures from 100 mJ, 100 fs, 0.8 micron laser data for (**a**) aluminum and (**b**) gold foils of varying thickness (dots with error bars). Diamonds with error bars are the weighed average for measurements at each thickness of both targets.

3. THEORETICAL AND NUMERICAL COMPARISON

Theoretically, the effective hot electron temperature that can be achieved by a linearly polarized light ultra-intense laser impinging on a solid density target was predicted to be approximately (Wilks *et al*., 1992; Wilks & Kruer, 1997):

$$T_{hot} \approx \left[\sqrt{\left(1 + \frac{I\lambda^2}{2.8 \times 10^{18}}\right)} - 1511\ (\text{keV})\right]. \qquad (1)$$

This equation shows that the hot electron temperature scales are roughly a square root of the laser intensity, and is about equal to the ponderomotive potential at the critical surface. In experiments, the electron temperatures can be somewhat lower due to factors including: realistic density profile effects (Lefebvre & Bonnaud, 1997; Fuchs *et al*., 1998), prepulse effects that change the incident laser profile (Adumi *et al*., 2004), collisional effects of the material, and other less than ideal conditions in a real experiment. Prepulse effects was discussed extensively with respect to the ponderomotive force driven skin layer acceleration SLA (Hora *et al*., 2002; Badziak *et al*., 2004*a*, 2004*b*; Hora, 2004; Osman *et al*., 2004; Badziak *et al*., 2005; Jablonski *et al*., 2005; Glowacz *et al*., 2006; Cang *et al*., 2005), these results are interesting for advanced fast ignitor schemes (Tabak *et al*., 1994; Deutsch, 2004; Bauer, 2003; Mulser & Bauer, 2004*a*; Mulser & Schneider 2004*b*).

https://doi.org/10.1017/S0263034605050585 Published online by Cambridge University Press

We performed a number of particles in cell (PIC) simulations (Langdon & Lasinski, 1976; Forslund *et al*., 1977) to gain insight into the physics of ultra-intense lasers interacting with thin targets. Figure 3 shows the phase space, *px* versus. *x*, of a thin slab of "solid" density plasma, (a) just after the laser pulse is incident, (b) just as the first wave of reflected electrons are reaching the front, and (c) after all hot electrons have been accelerated at least twice by the laser at the front of the target. They are one-dimensional (1D) with a "solid" density of $60n_{cr}$, (approximately 10^{21} cm^{-3} for 1 μm laser) with a thin strip (8 Å) of protons on both the front and back surfaces, to realistically represent the amount of energy that the electrons would lose as they reflux through the target, as this is a potentially important energy loss mechanism for electrons in this energy regime (50 keV–1.3 MeV). The front of the target has a slight gradient to represent a small amount of preformed plasma present from the laser prepulse. The laser energy is transferred to the background electrons and the ions via collisionless mechanisms. In the actual experiment, the energy in the low energy (< 5 keV) portion of the hot electron distribution function will transfer energy via collisions to either the background electrons, but for now, we concentrate on the high energy part of the spectrum. All collisionless methods for electrons to lose energy (usually associated with electrostatic fields such as TSNA, target normal sheath acceleration, and collisionless shocks) (Wilks *et al*., 2001) are contained in these simulations. For example, on each "bounce" at the boundaries, the electrons loss an amount of energy proportional to the ion-to-electron mass ratio (Glinsky *et al*., 1993).

By performing these computer simulations, it is possible to reproduce this dependence on thickness qualitatively and present a plausible argument as to why this behavior is observed in experiment. Early 1D and two-dimensional (2D) simulations suggested (Liang *et al*., 1998; Shen & Meyer-Ter-Vehn, 2001) that electron temperatures would be hotter, and maximum electron energy would be higher, if the electrons that were initially accelerated via the ponderomotive force could exit the back of the target, get pulled back into the target, due to the space charge effects, then get "re-accelerated" by the ponderomotive force at the front of the target again. This is commonly referred to as "reflexing," an example of which is shown in Figure 3a for the specific case of intensity corresponding to the experimental laser parameters as shown in Figure 2. It is clear from Figure 3b that electrons have not had time to return to the laser-plasma interface, and get reaccelerated, thus resulting in a smaller T_{hot}. Although this has long been suspected, this is the first direct experimental evidence that this phenomenon takes place in laser-target interactions. The fact that the temperatures are not exactly what is seen in the experiments is typical of the overestimates that PIC simulations give for electron temperatures, as collisional and full three-dimensional (3D) simulations, along with realistic equations of state are not employed here.

Several different methods to maximize the electron temperature for a given laser intensity was suggested (Liang *et al*., 1998; Shen & Meyer-Ter-Vehn, 2001; Silva *et al*., 2004). It turns out that an electron can obtain energy via this ponderomotive absorption (given by the value of Eq. (1)) every time that an electron passes through the accelerating region. This is due to the fact that if the electron phase in the acceleration region is just right, it can start at the bottom of the potential well, and go to the top, as the field oscillates and then is injected into the plasma (or solid.) If refluxing is considered, and if the electron loses only a small amount of energy to other processes, by collisions or other dissipative mechanisms, it will actually continue to be accelerated to a higher energy. However, the longer the laser pulse, the larger the number of energetic electrons there can be. Therefore, the present model of electron acceleration predicts a larger number of hot electrons, in addition to a hotter temperature. This is because the angular deflection of the electrons, as they reflux, increases, and they quickly propagate out of the spot and dump their energy around the laser focal spot. More cold electrons from the background solid (or

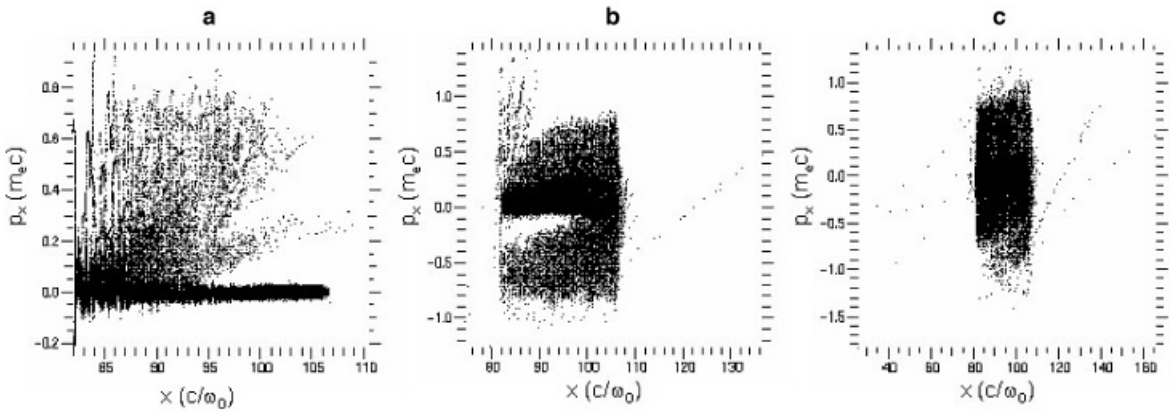

Fig. 3. Electron phase space at (**a**) early, (**b**) mid pulse, and (**c**) late (after laser pulse is finished) times. (**a**) Shows maximum velocities to ~ 0.8c. (**b**) Electrons from early accelerations are reflected at rear of target. Some of these have been "re-accelerated" at the front, and have higher energies than background electrons being accelerated at the same time. (**c**) After 2 circulations, the electrons are approaching a higher temperature than would result from just one acceleration.

https://doi.org/10.1017/S0263034605050585 Published online by Cambridge University Press

plasma) can come into the region, and pick up an amount of energy equal to the ponderomotive potential. This model is supported by recent experiments by Stephens *et al*. (2004).

An interesting prediction for this model of T_e being a function of target thickness is that ion acceleration will increase with thinner targets that satisfy $x_t/c < 2^*\tau_p$. It was proposed that a thin layer of protons can be efficiently accelerated off of the back of thin foils due to the electrostatic sheath that is set up by the hot electron "cloud" that surrounds the foil (Wilks *et al*., 2001; Davies, 2002; Pommier & Lefebvre, 2003; Sentoku *et al*., 2002). In fact, it was also shown that this TNSA proton acceleration mechanism predicts that the accelerating field increases as the square root of T_{hot}, where the scale length is taken to be the Debye length associated with the cloud of hot electrons. This predicts that as the target thickness decreases, the maximum ion energy that can be obtained for a given amount of energy will increase. This effect was observed in simulations discussed in Figure 3: thinner foils give higher proton energies. The resulting proton energies for the two cases of thick and thin targets are shown in Figure 4. It may be mentioned that there is a more general interest in the Debye sheath mechanisms even applied to the metallic state or nuclei (Hora *et al*., 1989, 2005; Hora, 2005; Osman *et al*., 2005).

4. DISCUSSION

Note that this is a related, but distinctly different, physical mechanism for increasing the peak proton energy to that discussed in MacKinnon *et al*. (2002), who first reported the observation of the increased proton energy effect experimentally. In this study, it was pointed out that the number of hot electrons increases during refluxing. Details concerning this effect were studied via simulations by Sentoku *et al.* (2002). It is certainly true that the number of hot electrons increases (n_{hot}), we find that the effective hot electron temperature (T_{hot}) also increases, thus, further enhancing the ion acceleration over thick slab experiments. Physically, the electron temperature increases because initially, the temperature is typically lower than the temperature predicted by Eq. (1) because the density on which the laser intensity acts on is typically many times critical. Because of this, both the n_{hot} and the effective T_{hot} that results are decreased. However, if the (somewhat) accelerated electrons that were accelerated are able to transit the thin foil while the laser pulse is still acting, some fraction of them can (potentially) gain more energy. If this happens many times (as in the case of a very thin foil) they can get accelerated even more. As more electrons are accelerated, the effective T_{hot} increases. This can continue until about twice the temperature as given in Eq. (1) is reached. At this point, only the number of hot electrons can increase. This is summarized in Figure 5, where it is seen that increasing the target thickness decreases the effective electron temperature up to a point. Past about 4 microns (for these parameters) the electron temperature is essentially unchanged, as electrons can no longer make the round trip through the solid while the laser is present on the front surface.

An interesting point is that if the intensity of the laser is sufficiently large, an ion shock can be produced on the front of the target which propagates to the back, disrupting the sharp density gradient needed for proton acceleration if the foil is too thin (Sentoku *et al*., 2002; Silva *et al*., 2004; Kaluza *et al*., 2004)

There are several effects relating to the inclusion of all three spatial dimensions that will modify this simple 1D model. Clearly, the inclusion of two more dimensions allows the electrons that many more degrees of freedom of motion, thus weakening the effect, if the transverse target dimension

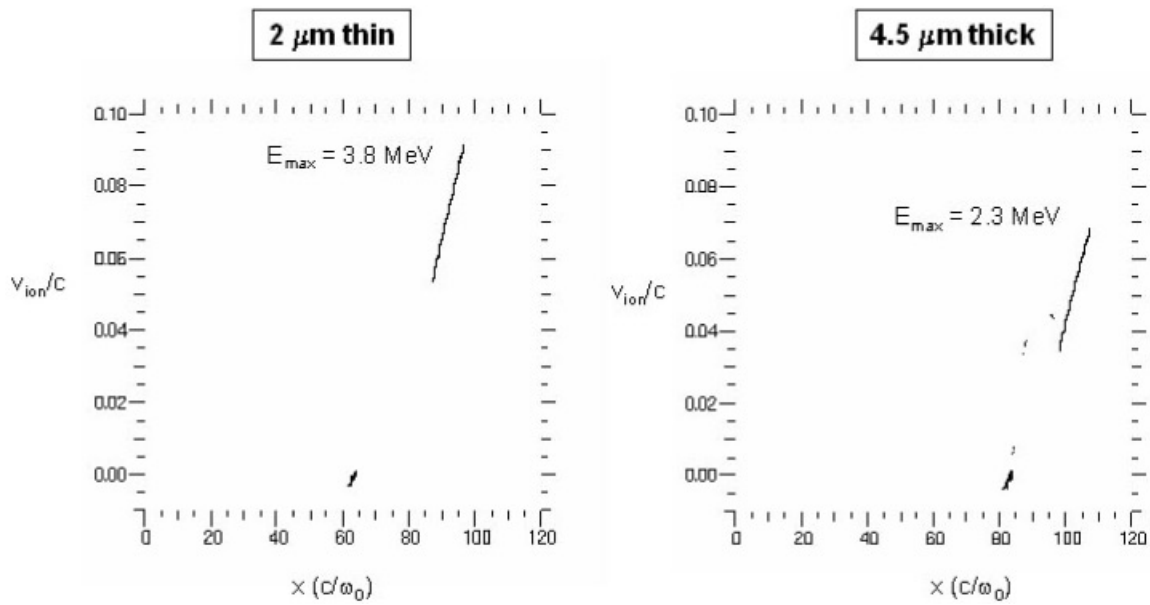

Fig. 4. Proton phase space showing thinner foils give higher energy protons than thicker foils do.

https://doi.org/10.1017/S0263034605050585 Published online by Cambridge University Press

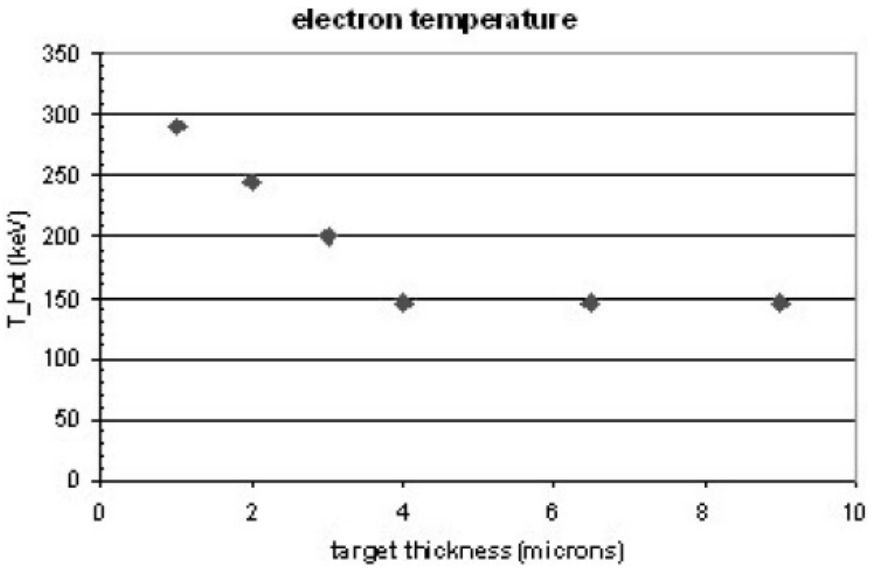

Fig. 5. The effective hot electron temperature T_{hot} versus target thickness as obtained from computer simulations showing hotter effective temperatures for thinner targets.

is much great than a typical hot electron mean free path in the material. Another effect not present in the PIC code is the effect of collisions on the path of the hot electrons. This is important since the range of a 50 keV electron, for example, in solid aluminum is approximately 20 μm. This implies that electrons below this energy would not get reaccelerated due to reflexing for a foil thicker than about 10 microns. For high Z materials, the effect extends to even higher energy electrons. In solid gold, the range for a 100 keV electron is approximately 15 μm. This implies that electrons below this energy due to reflexing for a foil thicker than about 7.5 microns would not receive any substantial increase in energy, since they would lose the initial energy they received from the laser during the time they transit the target. Clearly, as the thickness increases, and no reflexing is possible, the energy of the electrons should decrease simply due to the electrons losing energy as they propagate through the solid.

5. CONCLUSIONS

To conclude, it was shown experimentally that the hot electron temperatures generated by an ultra-intense laser pulse interacting with a solid target are determined by the thickness of the target. A physical model, based on theory and simulation, was proposed to explain this result. This information is useful for many applications of laser solid interactions (Pegoraro *et al.*, 2004; Roth *et al.*, 2001), where specific electron temperatures are required, and laser parameters is fixed.

ACKNOWLEDGMENTS

We gratefully acknowledge assistance of J. Boyett, and the support R. Al-Ayat, K. van Bibber, P. Beiersdorfer, J. Brase, M. Eckart, A. Ng, and B. Remington, as well as useful conversations with H.S. Park, P. Patel, R. Shepherd, W.L. Kruer, M. Key, R. Snavely, M. Allen, A. MacKinnon, and the entire short pulse team at LLNL. This work was performed under the auspices of the U.S. Department of Energy by the University of California, Lawrence Livermore National Laboratory under Contract No. W-7405-ENG-48 and LDRD No. 8918-31.

REFERENCES

Adumi, K., Tanaka, K.A., Matsuoka, T., Kurahashi, T., Yabuuchi, T., Kitagawa, Y., Kodama, R., Sawai, K., Suzuki, K., Okabe, K., Sera, T., Norimatsu, T. & Izawa, Y. (2004). Characterization of preplasma produced by an ultrahigh intensity laser system. *Phys. Plasmas* **11**, 3721–3725.

Badziak, J., Glowacz, S., Jablonski, S., Parys, P., Wolowski, J. & Hora, H. (2005). Generation of picosecond high-density ion fluxes by skin-layer laser-plasma interaction. *Laser Part. Beams* **23**, 143–148.

Badziak, J., Glowacz, S., Jablonski, S., Parys, P., Wolowski, J., Hora, H., Kraska, J., Laska, L. & Rohlena, K. (2004*a*). Production of ultrahigh ion current densities at skin-layer subrelativistic laser-plasma interaction. *Plasma Phys. Cont. Fusion* **46**, B541–B555.

Badziak, J., Glowacz, S., Jablonski, S., Parys, P., Wolowski, J. & Hora, H. (2004*b*). Production of ultrahigh-current-density ion beams by short-pulse skin-layer laser-plasma interaction. *Appl. Phys. Lett.* **85**, 3041–3043.

Bauer, D. (2003). Plasma formation through field ionization in intense laser-matter interaction. *Laser Part. Beams* **21**, 489–495.

Bonlie, J.D., Patterson, F., Price, D., White, B. & Springer, P. (2000). Production of $> 10^{21}$W/cm^2 from a large-aperture Ti : sapphire laser system. *Appl. Phys. B-Lasers Optics* **70**, S155–S160.

Chen, H., Patel, P.K., Price, D.F., Young, B.K., Springer, P.T., Berry, R., Booth, R., Bruns, C. & Nelson, D. (2003). A compact electron spectrometer for hot electron measurement in pulsed laser solid interaction. *Rev. Sci. Instr.* **74**, 1551–1553.

Davies, J.R. (2002). Proton acceleration by fast electrons in laser-solid interactions. *Laser Part. Beams* **20**, 243–253.

https://doi.org/10.1017/S0263034605050585 Published online by Cambridge University Press

Deutsch, C. (2004). Penetration of intense charged particle beams in the outer layers of precompressed thermonuclear fuels. *Laser Part. Beams* **22**, 115–120.

Forslund, D.W., Kindel, J.M. & Lee, K. (1977). Theory of hot-electron spectra at high laser intensity. *Phys. Rev. Lett*. **39**, 284–288.

Fuchs, J., Adam, J.C., Amiranoff, F., Baton, S.D., Gallant, P., Gremillet, L., Heron, A., Kieffer, J.C., Laval, G., Malka, G., Miguel, J.L., Mora, P., Pepin, H., & Rousseaux, C. (1998). Transmission through highly overdense plasma slabs with a subpicosecond relativistic laser pulse. *Phys. Rev. Lett.* **80**, 2326–2329.

Glinsky, M.E., Mason, R.J. & Tabak, M. (1993). Relativistic electrons and ion heating. *Bull. Am. Phys. Soc*. **38**, 2080.

Glowacz, S., Hora, H., Badziak, J., Jablonski, S., Cang, Yu & Osman, F. (2006). Suppression of the amplified spontaneous emission in chirped-pulse-amplification lasers by clean high-energy seed-pulse injection. *Laser Part. Beams*. In press.

Hora, H. (2004). Developments in inertial fusion energy and beam fusion at magnetic confinement. *Laser Part. Beams* **22**, 439–449.

Hora, H. (2005). Difference between relativistic petawatt-picosecond laser-plasma interaction and subrelativistic plasma-block generation. *Laser Part. Beams* **23**, 441–451.

Hora, H., Badziak, J., Boody, F., Höpfl, R., Jungwirth, K., Kralikowa, B., Kraska, J., Laska, L., Parys, P., Perina, V., Pfeifer, K. & Rohlena, J. (2002). Effects of ps and ns. laser pulses for giant ion source. *Optics Commun.* **207**, 333–338.

Hora, H., Miley, H.G. & Osman, F. (2005). Boltzmann equilibrium of endothermic heavy-nuclear synthesis in the Universe and a quark relation to the magic numbers. *Astrophys. Space Sci.* **293**, in press.

Hora, H., Gu, Min, Eliezer, S., Lalousis, P., Pease, R.S. & Szichman, H. (1989). Surface waves in laser produced plasma. *IEEE Trans. Plasma Sci.* **PS-17**, 284–294.

Itatani, J., Faure, J., Nantel, M., Mourou, G. & Watanabe, S. (1998). Suppression of the amplified spontaneous emission in chirped-pulse-amplification lasers by clean high-energy seed-pulse injection. *Opt. Commun.* **148**, 70.

Kaluza, M., Scheiber, J., Santala, M.I.K., Tsakiris, G.D., Eidmann, K., Meyer-Ter-Vehn, J. & Witte, K.J. (2004). Influence of the laser prepulse on proton acceleration in thin-foil experiments. *Phys. Rev. Lett.* **93**, 045003.

Kruer, W.L. & Wilks, S.C. (1992). Kinetic simulations of ultra-intense laser plasma interactions. *Plasma Phys. Contr. Fusion* **34**, 2061–2064.

Langdon, A.B. & Lasinski, B. (1976). Relativistic and electromagnetic particle-in-cell simulations. In: *Methods in Computational Physics* (Killen, J., Alder, B., Fernbach, S. & Rotenberg, M., Eds.) New York: Academic Press.

Lefebvre, E. & Bonnaud, G. (1997). Nonlinear electron heating in ultrahigh-intensity-laser-plasma interaction. *Phys. Rev. E* **55**, 1011–1014.

Liang, E.P., Wilks, S.C. & Tabak, M. (1998). Pair production by ultraintense lasers. *Phys. Rev. Lett*. **81**, 4887–4890.

MacKinnon, A.J., Sentoku, Y., Patel, P.K., Price, D.W., Hatchett, S., Key, M.H., Andersen, C., Snavely, R. & Freeman, R.R. (2002). Enhancement of proton acceleration by hot-electron recirculation in thin foils irradiated by ultraintense laser pulses. *Phys. Rev. Lett.* **88** (21).

Mulser, P. & Bauer, D. (2004*a*). Fast ignition of fusion pellets with superintense lasers: Concepts, problems, and perspectives. *Laser Part. Beams* **22**, 5–12.

Mulser, P. & Schneider, R. (2004*b*). On the inefficiency of hole boring in fast ignition. *Laser Part. Beams* **22**, 157–162.

Osman, F., Hora, H., Cang, Y., Evans, P., Cao, L.H., Liu, H., He, X.T., Badziak, J., Parys, A.B., Wolowski, J., Woryna, E., Jungwirth, K., Kralikova, B., Krasla, J., Laska, J., Pfeifer, M., Rohlena, K., Skala, J. & Ullschmied, J. (2004). Skin depth plasma front interaction mechanism with prepulse suppression to avoid relativistic self-focusing for high gain laser fusion. *Laser Part. Beams* **22**, 83–88.

Osman, F., Hora, H. & Ghahramany, N. (2005). Debye sheath mechanism at laser plasma interaction and generalization to nuclear forces and quark-gluon plasma. *Laser Part. Beams* **23**, 461–466.

Pegoraro, F., Atzeni, S., Borgehesi, M., Bulanov, S., Esirepov, T., Honrubia, J., Kato, Y., Khoroshkov, V., Nishihara, K., Tajima, T., Temporal, M. & Willi, O. (2004). Production of ion beams in high-power laser-plasma interactions and their applications. *Laser Part. Beams* **22**, 19–24.

Pommier, L. & Lefebvre, E. (2003). Simulations of energetic emission in laser-plasma interaction. *Laser Part. Beams* **21**, 573–581.

Roth, M., Cowan, T.E., Key, M.H., Hatchett, S.P., Brown, C., Fountain, W., Johnson, J., Pennington, D.W., Snavely, R.A., Wilks, S.C., Yasuike, K., Ruhl, H., Pegoraro, F., Bulanov, S.V., Campbell, E.M., Perry, M.D. & Powell, H. (2001). Fast ignition by intense laser accelerated proton beams. *Phys. Rev. Lett.* **86**, 436–439.

Sentoku, Y., Bychenkov, V.Y., Flippo, K., Maksimchuk, A., Mima, K., Mourou, G., Sheng, Z.M. & Umstadter, D. (2002). High-energy ion generation in interaction of short laser pulse with high-density plasma. *Appl. Phys. B-Lasers Optics* **74**, 207–215.

Shen, B.F. & Meyer-Ter-Vehn, J. (2001). High-density ($>$ $10(23)/cm^3$) relativistic electron plasma confined between two laser pulses in a thin foil. *Phys. Plasmas* **8**, 1003–1010.

Silva, L.O., Marti, M., Davies, J.R., Fonseca, R.A., Ren, C., Tsung, F.S. & Mori, W.B. (2004). Proton shock acceleration in laser-plasma interactions. *Phys. Rev. Lett.* **92** (1).

Stephens, R.B., Snavely, R.A., Aglitskiy, Y., Amiranoff, F., Andersen, C., Batani, D., Baton, S.D., Cowan, T. Freeman, R.R., Hall, T., Hatchett, S.P., Hill, J.M., Key, M.H., King, J.A., Koch, J.A., Koenig, M., MacKinnon, A.J., Lancaster, K.L., Martinolli, E., Norreys, P., Perelli-Cippo, E., Le Gloahec, M.R., Rousseaux, C., Santos, J.J. & Scianitti, F. (2004). K-alpha fluorescence measurement of relativistic electron transport in the context of fast ignition. *Phys. Rev. E* **69** (6).

Tabak, M., Glinsky, M.N., Kruer, W.L., Wilks, S.C., Woodworth, J., Campbell, E.M., Perry, M.D. & Mason, R.J. (1994). Ignition and high-gain with ultrapowerful lasers. *Phys. Plasmas* **1**, 1626–1634.

Wilks, S.C. & Kruer, W.L. (1997). Absorption of ultrashort, ultra-intense laser light by solids and overdense plasmas. *IEEE J. Quan. Electr*. **33**, 1954–1968.

Wilks, S.C., Kruer, W.L., Tabak, M. & Langdon, A.B. (1992). Absorption of ultra-intense laser-pulses. *Phys. Rev. Lett*. **69**, 1383–1386.

Wilks, S.C., Langdon, A.B., Cowan, T.E., Roth, M., Singh, M., Hackett, S., Key, M.H., Pennington, D., MacKinnon, A. & Snavelly, R.A. (2001). Energetic proton generation in ultra-intense laser-solid interactions. *Phys. Plasmas* **8**, 542–549.

https://doi.org/10.1017/S0263034605050585 Published online by Cambridge University Press